# Buoyancy induced mobility in two-phase debris flow

Shiva P. Pudasaini and Stephen A. Miller

Citation: AIP Conf. Proc. **1479**, 149 (2012); doi: 10.1063/1.4756084
View online: http://dx.doi.org/10.1063/1.4756084
View Table of Contents: http://proceedings.aip.org/dbt/dbt.jsp?KEY=APCPCS&Volume=1479&Issue=1
Published by the American Institute of Physics.

# Buoyancy Induced Mobility in Two-phase Debris Flow

Shiva P. Pudasaini* and Stephen A. Miller†

*Department of Geodynamics and Geophysics, Steinmann Institute, University of Bonn
Nussallee 8, D-53115, Bonn, Germany
†Department of Geodynamics and Geophysics, Steinmann Institute, University of Bonn

**Abstract.** This paper shows that buoyancy enhances mobility in two-phase debris flow with an analysis based on the generalized two-phase debris flow model proposed by Pudasaini [1]. The model (the most generalized two-phase flow model to date) incorporates many essential physical phenomena, including solid-volume-fraction-gradient-enhanced non-Newtonian viscous stress, buoyancy, virtual mass and a generalized drag force. We find a strong coupling between the solid- and the fluid-momentum transfer, where the solid normal stress is reduced by buoyancy, which in turn diminishes the frictional resistance, enhances the pressure gradient, and reduces the drag on the solid component. This leads to higher flow mobility. Numerical results show that the model can adequately describe the dynamics of buoyancy induced mobility in two-phase debris flows, and produces observable geometry of flowing mass in the run-out zone. The results presented here are consistent with the physics of the flow.

**Keywords:** Non-Newtonian Two-phase Flow, Debris Flow, Avalanche, Sediment Transport, Natural Hazards, Buoyancy, Flow Mobility
**PACS:** 45.70.Ht, 47.50.-d, 47.55.-t, 91.50.Xz, *91.62.Ty, 92.40.Vq, 92.40.Ha, 92.40.Gc

## INTRODUCTION

Debris flows are multiphase, gravity-driven flows consisting of randomly dispersed interacting phases. They consist of a broad distribution of grain sizes mixed with fluid. The rheology and flow behavior can vary and depends on the sediment composition and percentage of solid and fluid phases. Debris flows are extremely destructive and dangerous natural hazards, so there is a need for reliable methods for predicting the dynamics, runout distances, and inundation areas of such events. Significant research in the past few decades has focused on different aspects of single- and two-phase debris avalanches and debris flows [2,3,4,5,6,7,8,9], which was recently advanced by Pudasaini [1] in a comprehensive theory that accounts for the different interactions between the solid particles and the fluid. This model includes three fundamentally new and dominant physical aspects, including the solid-volume-fraction-gradient-enhanced non-Newtonian viscous stress, the virtual mass, and the generalized drag. The model constitutes the most generalized two-phase flow model to date, and can reproduce results from previous simple models that considered single- and two-phase avalanches and debris flows as special cases [2,3,5,6]. An important aspect of the new model is the influence of buoyancy in the flow dynamics, the run-out, and the depositional behavior. The equations are formulated as a set of well-structured, hyperbolic-parabolic model equations in conservative form [1].

To develop insight into the basic features of the complex and non-linear governing equations, the model is applied to simple, one-dimensional debris flow down an inclined channel which is abruptly connected to a horizontal run-out. This paper is mainly concerned about the influence of buoyancy on the flow mobility (longer travel distances) and the run-out behavior. The buoyancy effect on the overall dynamics of a two-phase debris flow is analyzed in detail. Simulation results demonstrate that buoyancy significantly affects on flow mobility and run-out morphology of two-phase debris flows, a result not yet available in literature. These results highlight the basic physics associated with buoyancy, with application to a wide range of two-phase geophysical mass flows, including particle-laden and dispersive flows, sediment transport, and debris flows. Simulation results are compatible with the physics of flow.

## A GENERAL TWO-PHASE DEBRIS FLOW MODEL

We consider the general two-phase debris flow model [1] reduced to one-dimensional channel flows. The depth-averaged mass and momentum conservation equations for the solid and fluid phases are:

*Numerical Analysis and Applied Mathematics ICNAAM 2012*
AIP Conf. Proc. 1479, 149-152 (2012); doi: 10.1063/1.4756084

$$\frac{\partial}{\partial t}(\alpha_s h)+\frac{\partial}{\partial x}(\alpha_s h u_s)=0,\quad \frac{\partial}{\partial t}(\alpha_f h)+\frac{\partial}{\partial x}(\alpha_f h u_f)=0, \tag{1}$$

$$\frac{\partial}{\partial t}\left[\alpha_s h\left(u_s-\gamma C\left(u_f-u_s\right)\right)\right]+\frac{\partial}{\partial x}\left[\alpha_s h\left(u_s^2-\gamma C\left(u_f^2-u_s^2\right)+\beta_s\frac{h}{2}\right)\right]=hS_s, \tag{2}$$

$$\frac{\partial}{\partial t}\left[\alpha_f h\left(u_f+\frac{\alpha_s}{\alpha_f}C\left(u_f-u_s\right)\right)\right]+\frac{\partial}{\partial x}\left[\alpha_f h\left(u_f^2+\frac{\alpha_s}{\alpha_f}C\left(u_f^2-u_s^2\right)+\beta_f\frac{h}{2}\right)\right]=hS_f, \tag{3}$$

in which $\beta_s=\varepsilon K p_{b_s}$, $\beta_f=\varepsilon p_{b_f}$, $p_{b_f}=-g^z$, $p_{b_s}=(1-\gamma)p_{b_f}$. In (2)-(3) the source terms are

$$S_s=\alpha_s\left[g^x-\frac{u_s}{|u_s|}\tan\delta\, p_{b_s}-\varepsilon p_{b_s}\frac{\partial b}{\partial x}\right]-\varepsilon\alpha_s\gamma p_{b_f}\left[\frac{\partial h}{\partial x}+\frac{\partial b}{\partial x}\right]+C_{DG}\left(u_f-u_s\right)|u_f-u_s|^{J-1}, \tag{4}$$

$$\begin{aligned}S_f=\alpha_f\Bigg[g^x-\varepsilon\Bigg[&\frac{1}{2}p_{b_f}\frac{h}{\alpha_f}\frac{\partial\alpha_s}{\partial x}+p_{b_f}\frac{\partial b}{\partial x}-\frac{1}{\alpha_f N_R}\left\{2\frac{\partial^2 u_f}{\partial x^2}-\frac{\chi u_f}{\varepsilon^2 h^2}\right\}\\&+\frac{1}{\alpha_f N_{R_A}}\left\{2\frac{\partial}{\partial x}\left(\frac{\partial\alpha_s}{\partial x}\left(u_f-u_s\right)\right)\right\}-\frac{\xi\,\alpha_s\left(u_f-u_s\right)}{\varepsilon^2\alpha_f N_{R_A}h^2}\Bigg]\Bigg]-\frac{1}{\gamma}C_{DG}\left(u_f-u_s\right)|u_f-u_s|^{J-1},\end{aligned} \tag{5}$$

where

$$C_{DG}=\frac{\alpha_s\alpha_f(1-\gamma)}{\left[\varepsilon U_T\{PF(Re_p)+(1-P)G(Re_p)\}\right]^J},\quad F=\frac{\gamma}{180}\left(\alpha_f/\alpha_s\right)^3 Re_p,\quad G=\alpha_f^{M(Re_p)-1},$$
$$\gamma=\frac{\rho_f}{\rho_s},\ C=\frac{1}{2}\left(\frac{1+2\alpha_s}{\alpha_f}\right),\ Re_p=\frac{\rho_f d\ U_T}{\eta_f},\ N_R=\frac{\sqrt{gL}H\rho_f}{\alpha_f\eta_f},N_{R_A}=\frac{\sqrt{gL}H\rho_f}{A\eta_f}. \tag{6}$$

Here, $x$ and $z$ are coordinates along the flow directions, and $g^x$ and $g^z$ are the components of gravitational acceleration. The solid and fluid constituents are denoted by the suffices $s$ and $f$, respectively. $h$ is the flow depth, and $u_s$ and $u_f$ are the solid and fluid velocities. $\rho_s$, $\rho_f$, and $\alpha_s$, $\alpha_f$ are the densities and volume fractions of the solid and the fluid, respectively. $L$ and $H$ are the typical length and depth of the flow, $\varepsilon=H/L$ is the aspect ratio, and $\mu=\tan\delta$ is the basal friction coefficient. $K$ is the earth pressure coefficient, $C_{DG}$ is the generalized drag coefficient, $J=1$ or $2$ represents the simple linear or quadratic drag. $U_T$ is the terminal velocity of a particle and $P\in[0,1]$ is a parameter which combines the solid-like ($G$) and fluid-like ($F$) drag contributions to flow resistance in two-phase debris flows. $p_{b_f}$ and $p_{b_s}$ are the effective fluid and solid pressures at the base. Here, $p_{b_s}$ is a buoyancy-reduced normal stress acting on the solids. $\gamma$ is the density ratio, $C$ is the virtual mass coefficient (solid particles induced kinetic energy of fluid phase), $\eta_f$ is the fluid viscosity, $M$ is a function of the particle Reynolds number ($Re_p$), $\chi$ includes vertical shearing of fluid velocity, and $\xi$ takes into account different distributions of solids volume fraction. $A=A(\alpha_f)$ is the mobility of the fluid at the interface, and $N_R$ and $N_{R_A}$ are quasi-Reynolds numbers associated with the classical Newtonian, and enhanced non-Newtonian fluid viscous stresses, respectively. The topography of the slope is represented by $b=b(x)$.

There are two important aspects of the model equations. (*a*) The inertial terms on the left hand side of (2)-(3) include the lateral pressures (associated with $\beta_s$ and $\beta_f$) and the virtual mass, $C$. (*b*) The source in the solid momentum (4) have three different contributions: (*i*) gravity, the Coulomb friction and the slope gradient (first square bracket); (*ii*) terms associated with the buoyancy force (second square bracket); and (*iii*) the generalized drag contribution ($C_{DG}$) (last term). The source terms for the fluid momentum equation, (5), have six different contributions. The first three terms emerge from the gravity load (first term), the term related to the fluid pressure gradient at the bed (second term) and the fluid pressure applied to the topographic gradient (third term), respectively. The fourth and fifth group of terms associated with $N_R$ and $N_{R_A}$ are the Newtonian viscous, and the solid-volume-fraction-gradient-enhanced non-Newtonian viscous stresses, respectively. The non-dimensional number $N_{R_A}$, which is also termed as the mobility number, is first obtained in [1]. Finally, the last term is due to the drag force.

The term associated with $\beta_s$ in the solid momentum equation (2) accounts for the buoyancy-reduced lateral pressure. The solid load is reduced by the buoyancy force by the factor $(1-\gamma)$ as seen in $p_{b_s}$, Coulomb friction and in the drag term, $C_{DG}$. The terms associated with the second square bracket in (4) are due to the buoyancy force that include free-surface and basal-surface gradients. For neutrally buoyant particles [10], the density ratio $\gamma\to 1$, and basal solid weight

$(p_{b_s})$ vanishes. Consequently, Coulomb friction disappears, lateral solid pressure gradient vanishes (because $\beta_s = 0$), the drag coefficient is zero, $C_{DG} = 0$, and that the basal slope effect on the solid phase also vanishes. In this limiting case, the only remaining solid force ($\alpha_s g^x$ in (4)) is due to gravity, and the force associated with buoyancy (the second square bracket in (4)). When $\gamma \to 0$, the flow does not experience any buoyancy effect. Then the effective frictional shear stress for the solid phase is that of the pure granular flows. The force due to pressure gradient is altered, the drag is high, and the effect of the virtual mass disappears in the solid momentum, and the left-hand side of (2) is purely inertial. All this leads to slowing down the motion. Neutrally buoyant flow is studied in [1]. Here, the contrasting scenario for flows between buoyant and non-buoyant flows are analyzed. In real two-phase flows of solid particles and fluid, naturally buoyant flow is physically more meaningful.

## NUMERICAL METHOD, SIMULATION SET-UP, RESULTS, DISCUSSIONS

The model (1)-(2) are written in well-structured standard conservative form of hyperbolic-parabolic partial differential equations. This facilitates numerical integration even when shocks are formed in field variables [6,9,11]. Model equations are solved in conservative variables $\mathbf{W} = \left(h_s, h_f, m_s, m_f\right)^t$, where $h_s = \alpha_s h$, $h_f = \alpha_f h$ are the solid and fluid contributions to debris height; and $m_s = \alpha_s h u_s$, $m_f = \alpha_f h u_f$, are the solid and fluid momentum fluxes. We implement the high-resolution shock-capturing Total Variation Diminishing Non-Oscillatory Central scheme [6,9,12,13,14]. We consider an inclined channel (slope angle, $\zeta = 45^\circ$) that is abruptly connected to a horizontal channel. The initial triangle is uniformly filled with homogeneous mixture of 65% solid and 35% fluid. Internal and basal friction angles of the solid-phase are $\phi = 35^\circ$ and $\delta = 25^\circ$. Other parameter values are: $\rho_f = 1,100$ kgm$^{-3}$, $N_R = 250,000$, $N_{R_A} = 50$, $Re_p = 1$, $U_T = 1, P = 0.5, J = 1, \chi = 3, \xi = 5, C = 0$. In order to simulate the influence of buoyancy, solid densities are taken to be $\rho_s = 2,500$ kgm$^{-3}$ and $\rho_s = 22,000$ kgm$^{-3}$, which correspond to the density ratios of $\gamma = 0.44$ and $\gamma = 0.05$. These values represent naturally buoyant flow and the flow in which buoyancy is almost neglected.

Buoyancy is an important aspect of two-phase debris flow, because it enhances flow mobility by reducing the frictional resistance, and other aspects of applied forces in the mixture. Buoyancy is present as long as there is fluid in the mixture. It reduces the solid normal stress, solid lateral normal stresses, and the basal shear stress by a factor $(1-\gamma)$. The effect is substantial when the density ratio $(\gamma)$ is large (natural debris flow). If the flow is naturally buoyant, e.g., $\gamma = 0.44$, the debris mass is fluidized and thus moves over longer travel distances (solid line, Fig. 1). Compared to a buoyant flow, the flow without buoyancy effect, i.e., $\gamma \to 0$ (dashed line), shows completely different behavior, for which travel distance is much shorter, and the deposition geometry is less realistic. The moment right after the mass hits the horizontal plane in shown in Fig. 1a, and Fig. 1b shows the (near) deposition behavior. It is observed in both panels that for naturally buoyant flows, the debris bulk mass is fluidized, the front moves substantially farther, the tail is long and lags behind. For $t = 6$ s, the overall flow height is also reduced in the tail side but with a strong head in the front, as observed in natural debris flow [3,6]. These are important results with regards to buoyancy in two-phase debris flows. As mentioned above, buoyancy is one of the main mechanisms responsible for decreasing the material strength and thus enhancing mass mobility, and actually controls the dynamics of the flow. With the effects of buoyancy, the debris head is thicker and followed by a long tail. These differences are substantial and are highlighted with respect to the important physical aspect of buoyancy. These simulations emphasize the need to consider buoyancy in two-phase debris flow because it plays a significant role in controlling the overall dynamics of debris-flow. Such a buoyancy-induced higher mobility and typical geometrical shape of the debris body as observed in the field is simulated here for the first time by a real two-phase debris flow model.

The non-dimensional ratio $\mathscr{M} = \mathscr{L}/\mathscr{H}$, where $\mathscr{L}$ is the effective horizontal flight and $\mathscr{H}$ is the vertical fall hight, is a measure of the flow mobility both measured from the front tip of the mass. The result is analyzed for $t = 6$ s. Here, $\mathscr{H} = 90$ m, and $\mathscr{L} \sim 215$ m, $\mathscr{L}_B \sim 315$ m, where $B$ stands for buoyancy. This gives flow mobilities of about $\mathscr{M} = 2.38$ (without buoyancy) and $\mathscr{M}_B = 3.5$ (with buoyancy). The angle of the energy line (joining the tip of initial mass and distal point of flow [14]) produced by the simulation, $\text{atan}(1/\mathscr{M}) \sim 23^\circ$, is close to the basal friction angle ($\delta = 25^\circ$). Similarly, $\text{atan}(1/\mathscr{M}_B) \sim 16^\circ$, which is almost the effective basal friction angle (appearing in the Coulomb friction term in (4)), $\text{atan}((1-\gamma)\tan\delta) = \text{atan}((1-0.44)\tan 25^\circ) \sim 15^\circ$. Therefore, the simulation results presented here are very consistent with the physics of flow. Also note that, there is about $10^\circ$ reduction in the effective friction angle due to buoyancy. This shows that, even for a small scale flow, buoyancy plays a substantial role in exceptionally mobilizing two-phase solid-fluid mixture flow. This indicates that for large scale mass flows [15], the effect of buoyancy can be much larger. Such an analysis is presented for the first time for the two-phase mass flow dynamics, which is here made

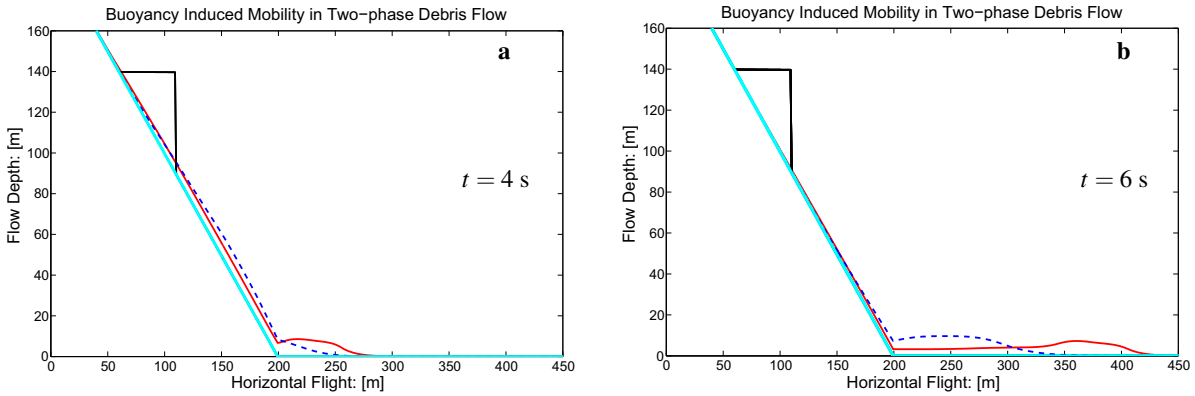


**FIGURE 1.** Buoyancy induces mobility in two-phase debris flow. The initial homogeneous mass (65% solid, 35% fluid) kept in a triangular shape, is suddenly released. The dashed line is the debris with density ratio $\gamma = 0.05$ (buoyancy neglected) while the solid line is with $\gamma = 0.44$ (naturally buoyant). **a**) The moment right after the mass hits the horizontal plane. Simulation with buoyancy is fundamentally different than without buoyancy, the front is much farther and moves as a well developed debris bulk. Due to the buoyancy induced higher mobility, the mass with buoyancy is much larger than the mass without buoyancy in the run-out zone. Flow without buoyancy is more resistive. So, the mass without buoyancy in the inclined channel is substantially larger than the mass with buoyancy in the same region. **b**) Deposition behavior is dynamically more important. The difference in actual run-out distances between the two simulations, with and without buoyancy, is very large. The run-out geometries are also completely different, one which includes buoyancy (solid line) produces more realistic run-out geometry as observed in debris flow in which the negligible front is diffused, followed by a fast growing front head that is again followed by a long tail.

possible due to underlying two-phase flow model.

## SUMMARY

This paper, which analyzes buoyant and non-buoyant flows, shows that buoyancy enhances flow mobility in two-phase debris flow. Simulation results demonstrate that buoyancy significantly affects the flow dynamics, and produces realistic run-out and depositional behaviors, and deposition morphology and mobility as observed in two-phase natural debris flows. Simulation results are compatible with the physics of flow. We hypothesize that buoyancy is a mechanism that controls the mobilization of two-phase mass flows, and thus proper modeling of two-phase debris-flow should include buoyancy.

## REFERENCES


1. S. P. Pudasaini, *J. Geophys. Res.*, doi:10.1029/2011JF002186 (2012).
2. S. B. Savage, and K. Hutter, *J. Fluid Mech.* **199**, 177–215 (1989).
3. R. M. Iverson, and R. P. Denlinger, *J. Geophys. Res.* **106**no.B1, 537–552 (2001).
4. S. P. Pudasaini, and K. Hutter, *J. Fluid Mech.* **495**, 193–208 (2003).
5. E. B. Pitman, and L. Le, *Phil. Trans. Royal Society* **A363**, 1573–1602 (2005).
6. S. P. Pudasaini, Y. Wang, and K. Hutter, *Nat. Hazards Earth Syst. Sci.* **5**, 799–819 (2005).
7. T. Takahashi, *Debris Flow: Mechanics, Prediction and Countermeasures*, Taylor & Francis Ltd., 2007.
8. E. D. Fernandez-Nieto, F. Bouchut, D. Bresch, M. J. Castro Diaz, and A. Mangeney, *J. Comput. Phys.* **227**, 7720-7754 (2008).
9. S. P. Pudasaini, *Phys. Fluids* **23**(4), 043301 (2011).
10. R. A. Bagnold, *Proc. R. Soc. Lond.* **A225**, 49–63 (1954).
11. S. P. Pudasaini, C. Kröner, *Physical Review E* **78**(4), 041308 (2008).
12. H. Nessyahu, and E. Tadmor, *J. Comput. Phys.* **87**, 408 (1990).
13. Y.-C. Tai, S. Noelle, J. M. N. T. Gray, and K. Hutter, *J. Comput. Phys.* **175**, 269–301 (2002).
14. S. P. Pudasaini, and K. Hutter, *Avalanche Dynamics: Dynamics of Rapid Flows of Dense Granular Avalanches*, Springer Berlin, New York, 2007, pp. 602.
15. F. Legros, *Engineering Geology* **63**(3), 301–331 (2002).